

**Geometrically enhanced extraordinary magnetoresistance in semiconductor-metal hybrids**

T. H. Hewett\* and F. V. Kusmartsev

*Department of Physics, Loughborough University, Loughborough LE11 3TU, United Kingdom*

(Received 25 August 2010; revised manuscript received 26 October 2010; published 13 December 2010)

Extraordinary magnetoresistance (EMR) arises in hybrid systems consisting of semiconducting material with an embedded metallic inclusion. We have investigated such systems with the use of finite-element modeling, with our results showing good agreement to existing experimental data. We show that this effect can be dramatically enhanced by over four orders of magnitude as a result of altering the geometry of the conducting region. The significance of this result lies in its potential application to EMR magnetic field sensors utilizing more familiar semiconducting materials with nonoptimum material parameters, such as silicon. Our model has been extended further with a geometry based on the microstructure of the silver chalcogenides, consisting of a randomly sized and positioned metallic network with interspersed droplets. This model has shown a large and quasilinear magnetoresistance analogous to experimental findings.

DOI: [10.1103/PhysRevB.82.212404](https://doi.org/10.1103/PhysRevB.82.212404)

PACS number(s): 75.47.-m, 72.20.My, 72.15.Gd

Since extraordinary magnetoresistance (EMR) was discovered in 2000,<sup>1</sup> improvements to magnetic field sensors have been considered.<sup>2</sup> This has been of particular interest in the area of ultrahigh-density magnetic recording. Future read heads based on the EMR effect have many potential advantages over existing devices based on giant magnetoresistance (GMR).<sup>3</sup> The EMR effect is particularly exciting with regards to its practical applications as significant values of magnetoresistance at room temperature and in low magnetic fields can be obtained. Where observed, these systems contain exclusively nonmagnetic materials in their construction therefore achieving a high signal-to-noise ratio.<sup>3</sup> Here, we present findings that have the potential to extend the EMR effect to a wider range of semiconducting materials via a huge geometrical enhancement. We also look at the link between the EMR effect and the large, linear, and unsaturating magnetoresistance discovered in the silver chalcogenides<sup>4</sup> with the use of a random branch and droplet model (RBDM).

EMR was initially discovered in modified van der Pauw disks consisting of a high mobility narrow gap semiconducting outer disk (InSb of radius  $r_b$  with  $\sigma_0=1.86 \times 10^4$  1/ $\Omega$  m and  $\mu=45\,500$  cm<sup>2</sup>/V s) with an embedded metallic inclusion (Au of radius  $r_a$  with  $\sigma_0=4.52 \times 10^7$  1/ $\Omega$  m and  $\mu=50$  cm<sup>2</sup>/V s). The filling factor,  $\alpha$ , can be defined as  $\alpha=r_a/r_b$ . Magnetoresistance values of over one million percent were reported at room temperature in an applied magnetic field of 5 T for a system with  $\alpha=13/16$ .<sup>1</sup> The extremely large magnetoresistance values arise from the redistribution of current paths throughout the system as a perpendicular magnetic field is applied. This current redistribution appears from the Lorentz force acting on the charge carriers, creating a Hall angle that approaches 90° in large magnetic fields. This leads to two regimes: one of low resistance at low fields (short circuit), here the majority of the current flows through the metallic region; the other of high resistance at high fields (open circuit), here the current is expelled from the metallic region and is forced to flow around the outer semiconducting material of much higher resistance. Since its discovery, EMR has been shown to arise in various experimental systems,<sup>5,6</sup> including linear devices produced via conformal mapping.<sup>7</sup>

Using the finite-element method via COMSOL MULTIPHYSICS (Ref. 8) the EMR effect found by Solin *et al.*<sup>1</sup> has been modeled and the mechanism verified. In order to replicate the experimental system<sup>1</sup> as precisely as possible we created a two-dimensional (2D) model with the transverse magnetic field included by the 2D magnetoconductivity tensor,

$$\sigma_{ij} = \frac{\sigma_0}{1 + (\mu H)^2} \begin{pmatrix} 1 & -\mu H \\ \mu H & 1 \end{pmatrix}. \quad (1)$$

Four point contacts were included around the disk perimeter; two contacts inject the current into the system while the other two were used to measure the change in electrical potential. This allowed the magnetoresistance to be calculated using the standard definition,

$$\frac{\Delta R}{R_0} = \frac{R(H) - R(0)}{R(0)}. \quad (2)$$

Our model produced results that agree well with the experimental data,<sup>9</sup> Fig. 1 shows how the magnetoresistance varies with  $\alpha$  for five values of magnetic field. In general we see good agreement with experiment. However, experimentally there is a peak in the magnetoresistance at  $\alpha=13/16$ . Our results do not exhibit this peak and we see a monotonic growth with filling factor. This can be explained by the difference between our model and the experimental system. Experimentally the contacts have a finite size on the disks perimeter; our model however assumes point contacts. This difference becomes more apparent with larger filling factors and in high magnetic fields as the semiconducting channels become narrower and are forced to carry a larger proportion of the current.

The EMR mechanism can be supported by looking at the current distribution throughout the systems, see Figs. 3(a) and 3(b). Here, with no magnetic field applied to the system the majority of the current flow is directed through the conducting droplet. The application of a magnetic field then leads to a very clear expulsion of current from the metallic region forcing the current to flow through the semiconducting outer disk. Larger filling factors generally produce larger magnetoresistance values; this is due to the outer semicon-

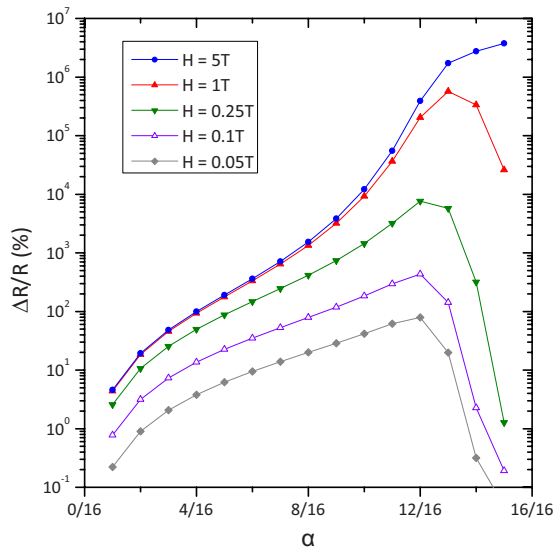


FIG. 1. (Color online) Magnetoresistance as a function of filling factor ( $\alpha$ ) at five values of magnetic field;  $H=0.05$  (black  $\blacklozenge$ ),  $0.1$  (purple  $\triangle$ ),  $0.25$  (green  $\blacktriangledown$ ),  $1$  (red  $\blacktriangle$ ), and  $5$  T (blue  $\bullet$ ) for systems based on the experimental geometry by Solin *et al.* (Ref. 1). The system geometry consists of an outer semiconducting disk (of radius  $0.5$  mm) containing an embedded circular metallic inclusion, including four equally spaced contacts on the perimeter [see Fig. 2(a)].

ducting disk becoming proportionally narrower. At low magnetic fields the current passes through shorter distances of semiconductor while at large fields the current is forced to flow along long paths through these narrow semiconducting channels, enhancing the magnetoresistance.

The EMR effect is strongly dependent on the geometry of the system; unlike many other magnetoresistance effects the geometrical component of the magnetoresistance is larger than the physical one.<sup>1</sup> This geometrical contribution depends not only on the shapes of the conducting and semiconducting material but also on the positions of the contacts in the system.<sup>10</sup> As a result, our model was adapted in order to investigate the effect of the system geometry on the magnetoresistance. To enhance the magnetoresistance the difference between the low and high resistance regimes is required to be a maximum. The geometry in which the largest magnetoresistance value was obtained contained a multibranched metallic inclusion; see Fig. 2(b). This geometry shows a four order of magnitude increase in magnetoresistance over the experimental geometry containing a circular metallic droplet of the same filling factor (see Fig. 2). Many geometries were investigated with such multibranched geometry [as in Fig. 2(b)] showing the largest enhancement. We do not believe this geometry to be the most optimal configuration and other multibranched geometries may show further enhancement. However, the significant result is in showing that such huge enhancements can be achieved by modification of the system geometry.

When this multibranched geometry (with  $\alpha=0.5$ ) is compared to geometries containing circular metallic regions of larger filling factors (for example,  $\alpha=15/16$ ) the enhancement is less dramatic, being only approximately two orders

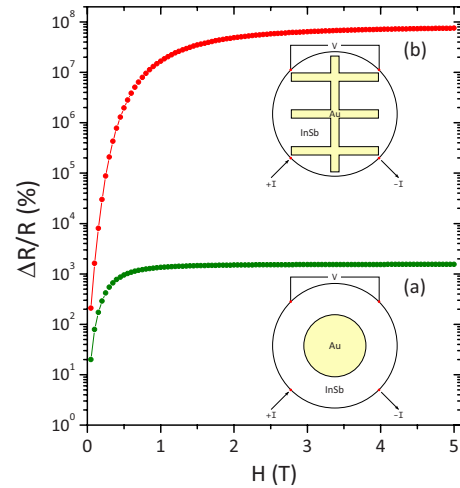


FIG. 2. (Color online) Magnetoresistance as a function of applied magnetic field for two system geometries (metal regions shown in yellow, semiconducting regions shown in white, including four point contacts, two for current and two for electric potential): (a) the experimental geometry, based on the experimental systems by Solin *et al.* (Ref. 1); (b) a modified geometry containing a multi-branched metallic inclusion in which we see a four order of magnitude increase in magnetoresistance over the case in (a). Both systems contain the same proportion of conducting to semiconducting material ( $\alpha=0.5$ ) with the disk radius being  $0.5$  mm in each case.

of magnitude. This comparison is useful as the low- and high-field regimes have a similar composition for such filling factors. The idealized current path in zero field is a straight line from the contacts to the nearest point in the metallic region, creating the lowest resistance path. However, the idealized high magnetic field regime is one where the current flow is directed around the disk periphery of much more resistive semiconducting material.

In order to understand this geometrical enhancement we look to the current distribution in the system, see Figs. 3(c) and 3(d). Here, we see that the current distribution is more diverse and complex than the one we found<sup>9</sup> for systems containing circular metallic droplets as in experiments by Solin *et al.*<sup>1</sup> [Figs. 3(a) and 3(b)] but in general the same mechanism can be observed. From the current streamlines we see that in all cases the current flow is highly inhomogeneous and changes significantly with magnetic field. Without magnetic field the current direction is always perpendicular to the metallic surface and the majority of the current flows through the metal. The new system geometry means that the low resistance path has an extremely low resistance. The majority of the current flows through the lower horizontal bar [as indicated in Fig. 3(c) where the large horizontal black arrows indicate the largest current flow] with only an extremely small fraction of the current path passing through semiconducting material. The high-field limit [see Fig. 3(d)] also enhances the magnetoresistance due to the geometry. The application of a magnetic field forces an increasing proportion of the current to flow through the semiconductor. In large fields the current is tangential to the metallic surface with the current thus avoiding the metal. The path the current takes in the semiconductor is lengthy and becomes extremely

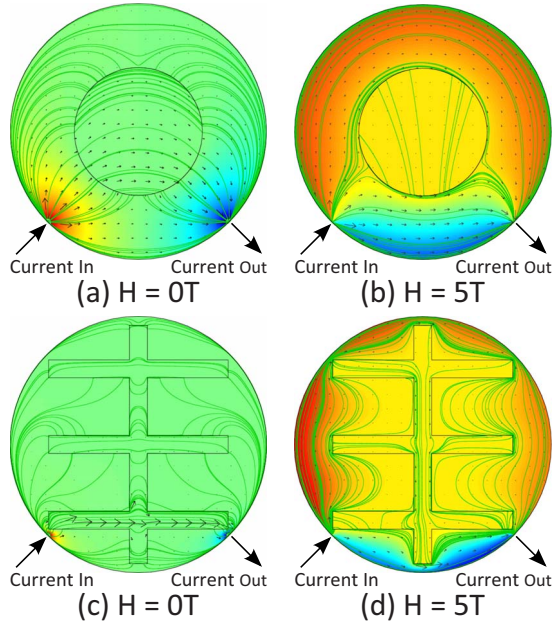


FIG. 3. (Color online) Here, we consider the same samples as in Fig. 2. The background color shows the value of the electric potential. The minimums (shown in blue) correspond to (a)  $-0.6$  mV, (b)  $-12$  mV, (c)  $-0.25$  mV, and (d)  $-10$  mV while the maximums (shown in red) correspond to (a)  $0.6$  mV, (b)  $6$  mV, (c)  $0.25$  mV, and (d)  $6$  mV. The metal regions [yellow in (b) and (d) and green in (a) and (c)] have zero potential. The change in potential scales continuously with color. Without magnetic field [see (a) and (c)] the major changes in potential arise around the current contacts. With magnetic field [ $H=5$  T, see (b) and (d)] we see changes in potential are huge. The streamline plot (green lines) indicates the local direction of the current flow. The length of the arrows (black) indicates the amplitude of the current at a particular point where the arrow originates.

narrow at various points. The fact that the current is forced along long paths through these narrow channels of semiconducting material enhances the magnetoresistance dramatically. However, this multibranch structure does lead to an increase in the magnetic field at which the magnetoresistance saturates. The geometry in Fig. 2(a) shows saturation in magnetic fields on the order of 1 T. The multibranch structure in Fig. 2(b) does not show saturation until fields of approximately 3 T. The geometrical enhancement of the magnetoresistance is more significant at higher magnetic fields.

The semiconductor used experimentally (and in these models) is InSb; a high mobility narrow gap semiconductor. The effect of the semiconductor mobility is to adjust the magnetic field at which the magnetoresistance saturates. Low mobility semiconductors have been shown to produce small magnetoresistance values, such as silicon EMR devices based on the linear external shunt geometry.<sup>11</sup> However, we suggest that such low mobility semiconductors, for example Si or Ge, could produce EMR devices with a similarly large magnetoresistance to those found by Solin *et al.*<sup>1</sup> in combination with the geometrical enhancement reported here. Silicon has far from ideal material parameters for the EMR effect, yet it could show significant benefits for applications due to its practical convenience. If such devices that exhibit

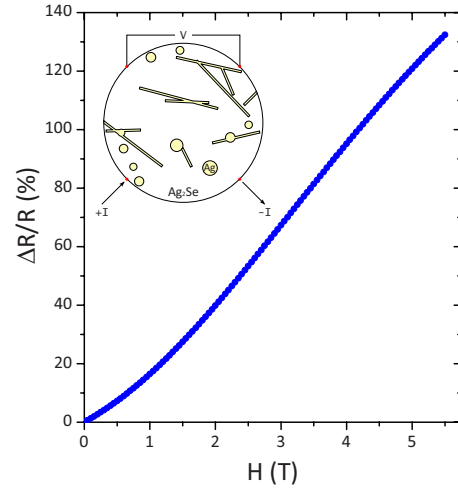


FIG. 4. (Color online) Magnetoresistance as a function of magnetic field ( $H$  up to 5.5 T as in experiment) for a RBDM geometry (see inset). Metal regions are shown in yellow and semiconducting regions shown in white (including four point contacts, two for current and two for electric potential). The model contains conducting branches and droplets with their sizes and positions determined by random numbers mimicking the microstructure of the silver chalcogenides where excess silver has been shown to form a percolating network along grain boundaries. The magnetoresistance has a quasi-linear dependence on magnetic field as observed experimentally in the silver chalcogenides. Here  $\alpha=0.29$  with the disk radius being  $0.5 \mu\text{m}$ , with purely diffusive transport considered.

large magnetoresistance values are to be produced the appearance of a Schottky barrier should be considered in design. The semiconductor-metal interface is required to be Ohmic in behavior; the formation of a Schottky barrier would decrease the resulting EMR effect. Finite-element modeling has been used previously to investigate the EMR effect.<sup>12,13</sup> However, investigating the effect of the system geometry in this way is unique.

The silver chalcogenides, for example,  $\text{Ag}_{2+\delta}\text{Se}$  and  $\text{Ag}_{2+\delta}\text{Te}$ , are another example of a large magnetoresistance effect arising in semiconductor-metal hybrid systems. With  $\delta=0$ , the materials are semiconducting. However, a small excess ( $\delta$ ) of silver added to the materials caused a large, linear, and unsaturating magnetoresistance.<sup>4</sup> The microstructure of these materials has been documented,<sup>14,15</sup> where the excess silver forms a branched silver network (forming along grain boundaries) with silver droplets interdispersed in the semiconducting material. This two-phase nature is analogous to the EMR effect and based on these findings we have created a RBDM. This model was created in order to mimic the microstructure of the silver chalcogenides with randomly sized, positioned, and orientated branches and droplets. This model contains an equal filling factor for both branches and droplets, with the total filling factor,  $\alpha=0.29$ . The material parameters used in this model are now given: semiconducting  $\text{Ag}_2\text{Se}$  has  $\sigma_0=5 \times 10^4$   $1/\Omega\text{m}$  with  $\mu=2500$   $\text{cm}^2/\text{Vs}$  while the excess silver has  $\sigma_0=6.62 \times 10^7$   $1/\Omega\text{m}$  with  $\mu=70$   $\text{cm}^2/\text{Vs}$ .

Figure 4 shows the magnetoresistance as a function of magnetic field for the RBDM geometry. Here, we see a qua-

silinear dependence on magnetic field. The silver chalcogenides contain a much larger and more complex formation of conducting structures without an equal area of metal forming branches and droplets. We believe that averaging many possible configurations would produce a more linear response. The magnitude of the effect is significantly smaller than that found in the modified van der Pauw disk geometry [Fig. 2(a)]. This is due to the low mobility of the semiconductors in these materials and the fact that the conducting regions occur in small disjointed fragments. The magnitude of the magnetoresistance given in Fig. 4 is in very good agreement with the experimental data (at room temperature). This RBDM geometry appears to have similarities to other theoretical models<sup>16</sup> including a random resistor network that has also shown to exhibit a linear magnetoresistance.<sup>17</sup>

Here, we have formed a model able to reproduce experimental EMR results with good agreement. This model has enabled the mechanism behind the effect to be further investigated and established with the use of current flow diagrams. This model was then developed to investigate the effect of the system geometry on the magnetoresistance. The magnetoresistance was found to be enhanced by over four orders of magnitude for a geometry containing a multibranching metallic region. This enhancement could be practically significant as it may allow for other semiconducting materials, with less ideal material parameters, for example, silicon, to be used in EMR devices. Finally, a RBDM geometry was utilized in an attempt to replicate the large, linear and unsaturating magnetoresistance found in the silver chalcogenides. Our model shows a quasilinear response of the same magnitude as in experiments.

---

\*t.h.hewett@lboro.ac.uk

<sup>1</sup>S. A. Solin, T. Thio, D. R. Hines, and J. J. Heremans, *Science* **289**, 1530 (2000).

<sup>2</sup>S. A. Solin, *Sci. Am.* **291**, 70 (2004).

<sup>3</sup>S. A. Solin, D. R. Hines, A. C. H. Rowe, J. S. Tsai, Y. A. Pashkin, S. J. Chung, N. Goel, and M. B. Santos, *Appl. Phys. Lett.* **80**, 4012 (2002).

<sup>4</sup>R. Xu, A. Husmann, T. F. Rosenbaum, M.-L. Saboungi, J. E. Enderby, and P. B. Littlewood, *Nature (London)* **390**, 57 (1997).

<sup>5</sup>J. Suh, W. Kim, J. Chang, S.-H. Han, and E. K. Kim, *J. Korean Phys. Soc.* **55**, 577 (2009).

<sup>6</sup>C. H. Möller, O. Kronenwerth, D. Grundler, W. Hansen, Ch. Heyn, and D. Heitmann, *Appl. Phys. Lett.* **80**, 3988 (2002).

<sup>7</sup>T. Zhou, D. R. Hines, and S. A. Solin, *Appl. Phys. Lett.* **78**, 667 (2001).

<sup>8</sup>COMSOL MULTIPHYSICS, Version 3.4, 2007.

<sup>9</sup>T. H. Hewett and F. V. Kusmartsev, *Int. J. Mod. Phys. B* **23**,

4158 (2009).

<sup>10</sup>C.-B. Rong, H.-W. Zhang, J.-R. Sun, and B.-G. Shen, *Appl. Phys. Lett.* **89**, 052503 (2006).

<sup>11</sup>A. S. Troup, D. G. Hasko, J. Wunderlich, and D. A. Williams, *Appl. Phys. Lett.* **89**, 022116 (2006).

<sup>12</sup>J. Moussa, L. R. Ram-Mohan, J. Sullivan, T. Zhou, D. R. Hines, and S. A. Solin, *Phys. Rev. B* **64**, 184410 (2001).

<sup>13</sup>M. Holz, O. Kronenwerth, and D. Grundler, *Phys. Rev. B* **67**, 195312 (2003).

<sup>14</sup>M. von Kreutzbruck, B. Mogwitz, F. Gruhl, L. Kienle, C. Korte, and J. Janek, *Appl. Phys. Lett.* **86**, 072102 (2005).

<sup>15</sup>M. von Kreutzbruck, G. Lembke, B. Mogwitz, C. Korte, and J. Janek, *Phys. Rev. B* **79**, 035204 (2009).

<sup>16</sup>S. A. Bulgadaev and F. V. Kusmartsev, *Phys. Lett. A* **342**, 188 (2005).

<sup>17</sup>M. M. Parish and P. B. Littlewood, *Nature (London)* **426**, 162 (2003).